
Ultraflexible electrode arrays for months-long high-density electrophysiological mapping of thousands of neurons in rodents

In the format provided by the authors and unedited

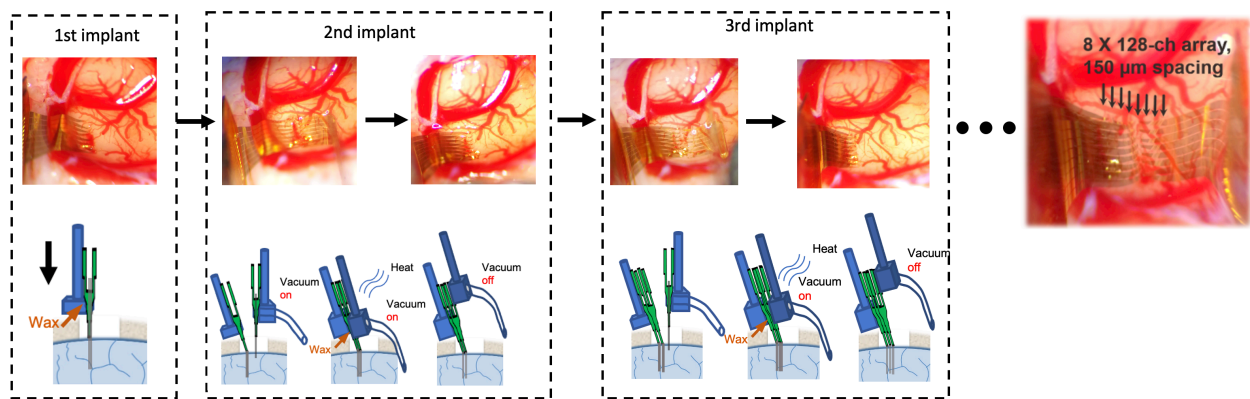
Supplementary Tables 1 and 2
Supplementary Figs. 1–7
Captions for Supplementary Videos 1–7

Supplementary Table 1 | Summary of animals in the experiments

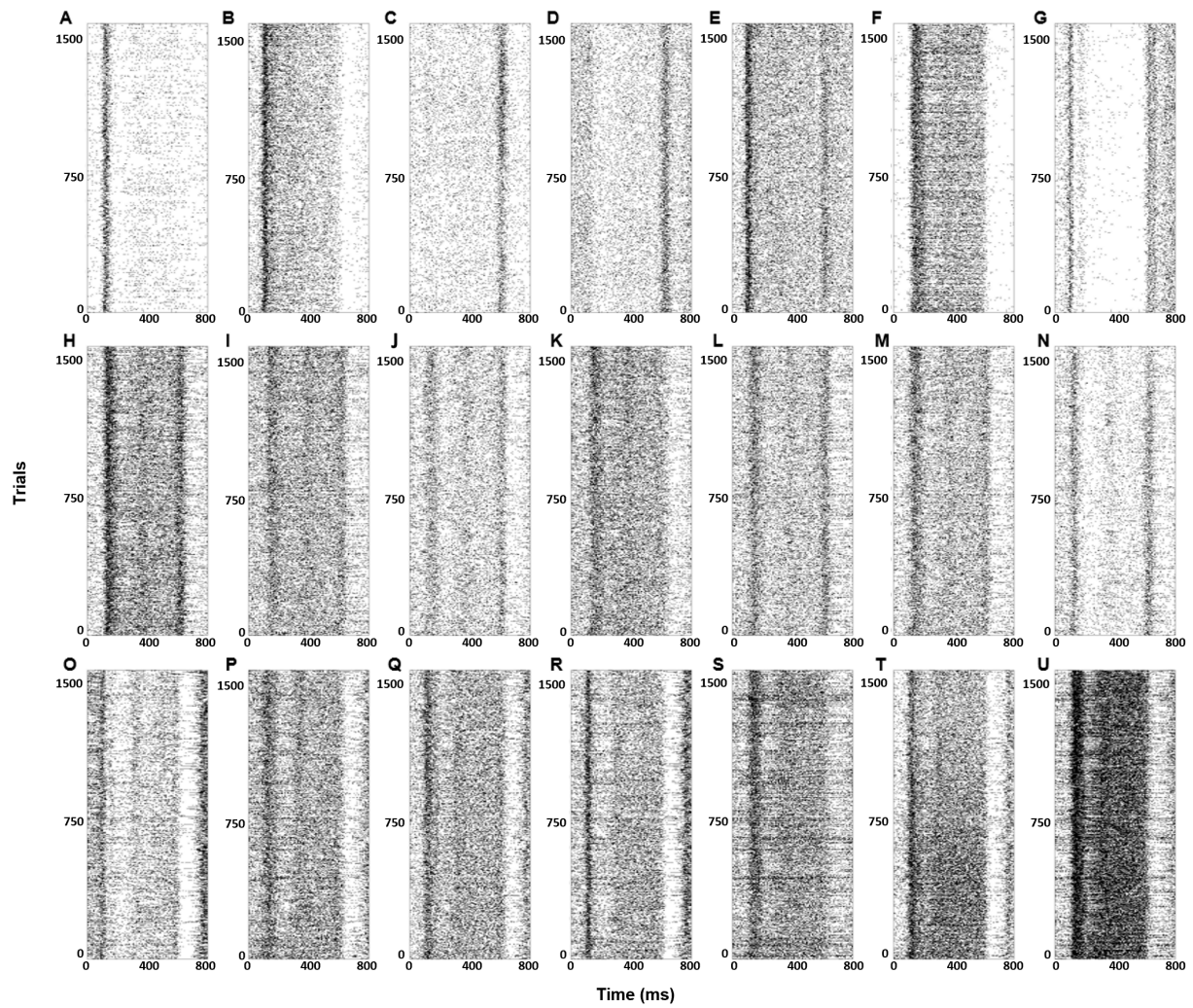
Animal #	Model (quantity)	Implants	Implantation site	Inter-module spacing	Recording duration	Figures
1	Rat	Type I (8 modules)	Primary visual cortex (V1, 3-4 ML, -(7-8) AP, 0-1 DV)	150 μm	1 month	Fig. 2a and 2c
2	C57B6	Type I (10 modules)	Visual area (LM, V1 and PM, 1-4.7 ML, -(2.3-3.8) AP, 0-1 DV)	200 μm	1.5 months	Fig. 2c, 3 and 4
3	Thy1-mhChR2-EYFP	Type I (8 modules)	Primary visual cortex (V1, 2-3 ML, -(2-3) AP, 0-1 DV)	150 μm	3 months	Fig. 2c and 5
		Optical fiber ($\text{\O}150 \mu\text{m}$) *30° to the brain surface	Primary visual cortex (V1, 3.5 ML, -2.75 AP, 0.5 DV)			
4	CD1	Type I (18 modules)	Motor cortex ($\pm(0.5-2)$ ML, 1.2-2.4 AP, 0-1 DV), sensory cortex ($\pm(2.5-3.5)$ ML, -(0.8-2) AP, 0-1 DV) and visual cortex ($\pm(2-3)$ ML, -(2.4-3.6) AP, 0-1 DV)	150-600 μm within each region	5 months	Fig. 2c, 6, and 7a-j
5	CD1	Type I (5 modules)	Motor cortex ($\pm(0.5-3)$ ML, 1.2-2.6 AP, 0-1 DV), sensory cortex ($\pm(2.5-3.5)$ ML, -(0.8-2) AP, 0-1 DV)	300-600 μm within each region	10 months	Fig. 2c and 7a-d
6	C57B6	Type I (mouse: 8 modules)	Visual area (LM and V1, 2-3 ML, -(2.5-3.1) AP, 0-1 DV)	200 μm	For MicroCT	Fig. 1a
7	Rat	Type I (rat: 8 modules)	Visual area (LM and V1, 2.5-3.5 ML, -(6-7) AP, 0-1 DV)	200 μm	For MicroCT	Fig. 1e

Supplementary Table 2 | Hyperparameters for LSTM

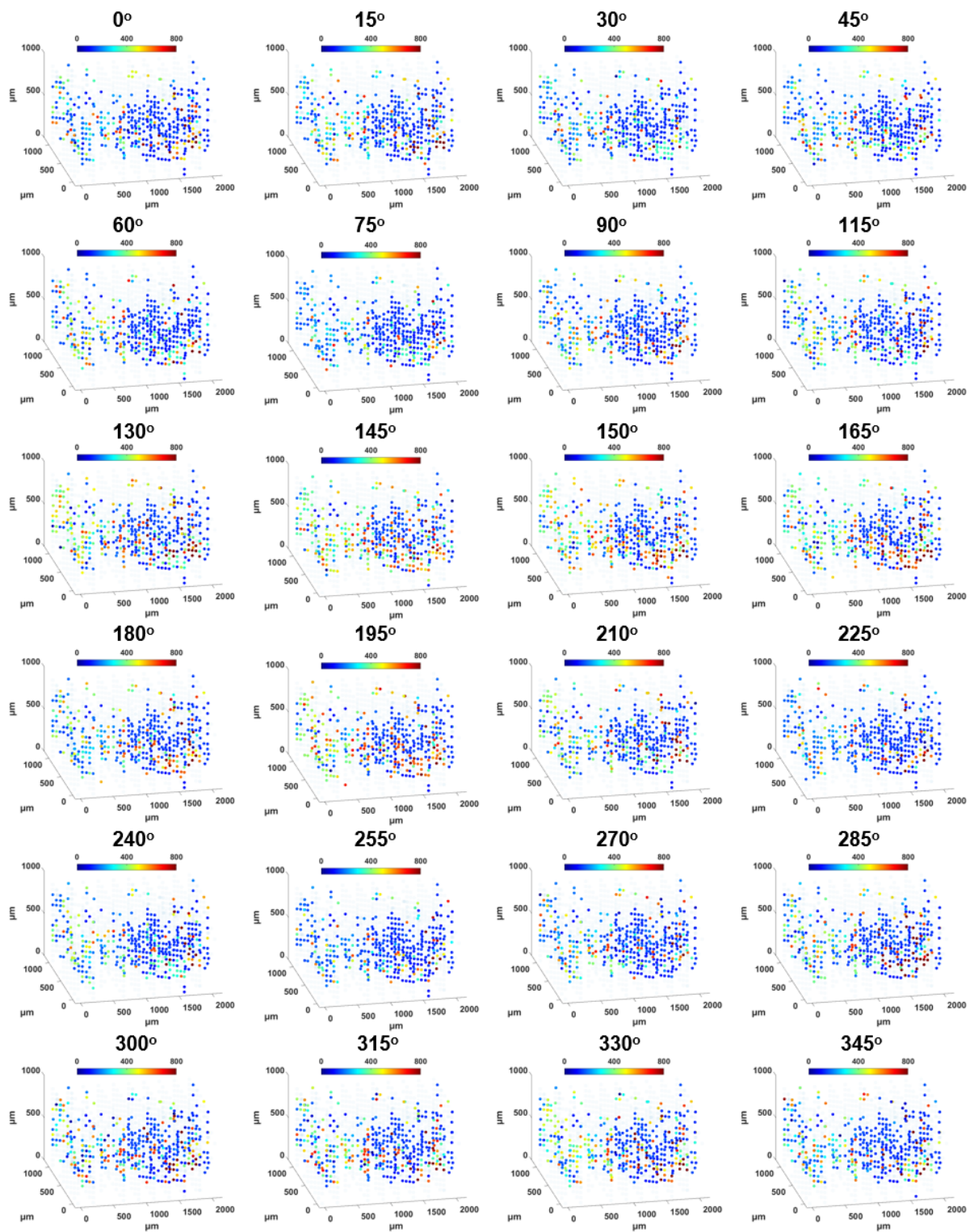
Hyperparameter	Range Searched
Number of training epochs	$[2^1 \quad 2^5]$
Dropout rate LSTM recurrent and output layer	$[2^{-5} \quad 2^{-1}]$
Dropout rate LSTM input layer	$[2^{-5} \quad 2^{-1}]$
Number of LSTM cells	$[10^{1.5} \quad 10^{3.1}]$
Learning rate of RMSprop optimizer	$[10^{-4.5} \quad 10^{-2}]$
Rho of RMSprop optimizer	$[2^{-1} \quad 2^{-0.15}]$
Batch size	128 (fixed based on computing capacity)



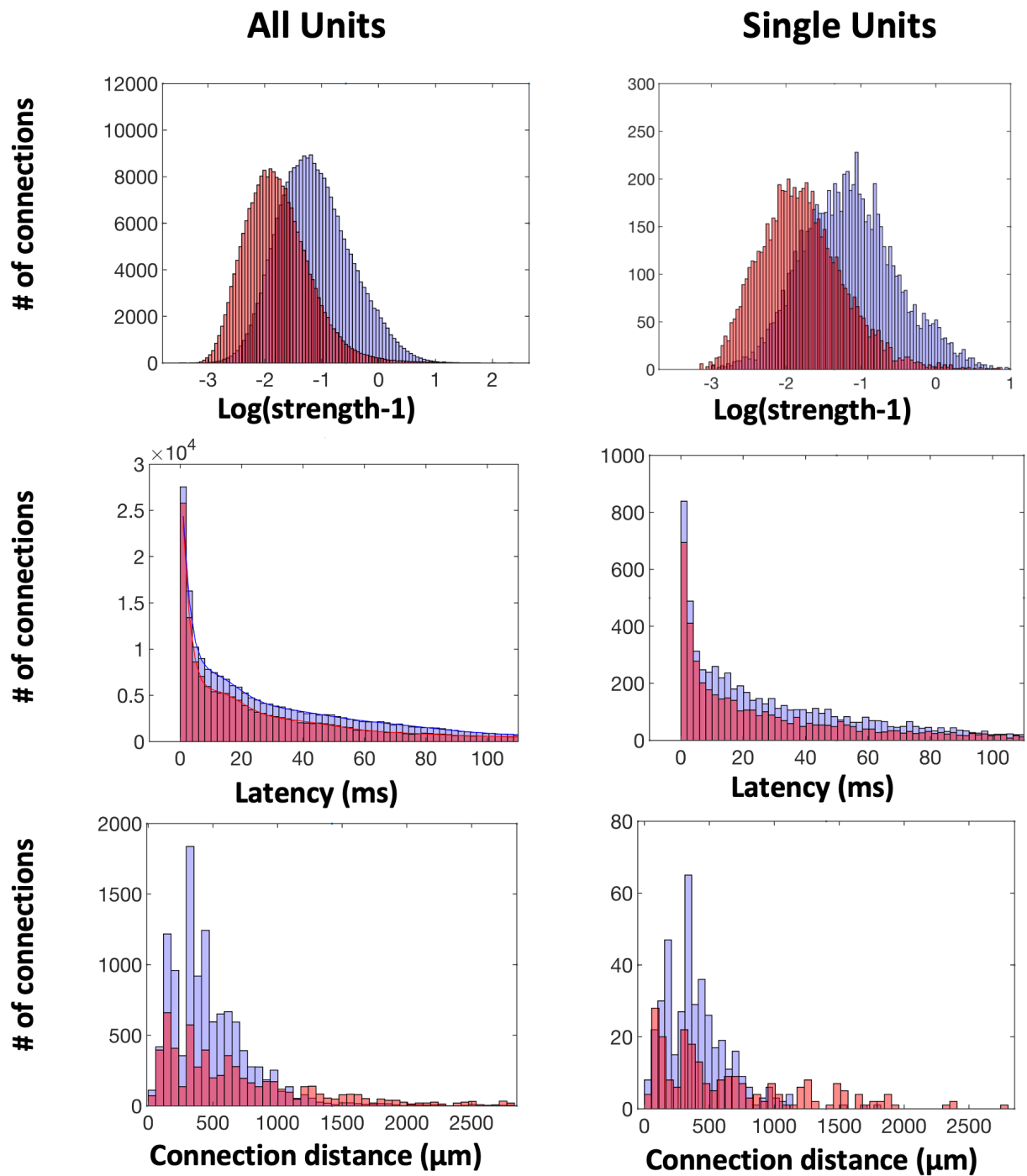
Supplementary Fig. 1 | Typical implantation procedure for 3D NET arrays. Assembled NET modules were implanted sequentially into the brain using a pair of stereotaxic micromanipulators, one module at a time in a similar manner as previously described. In this example, a rat brain was implanted with 8 NET-modules at a targeted module distance of 150 μm . Arrows in the last photo denote the implantation location of each NET module.



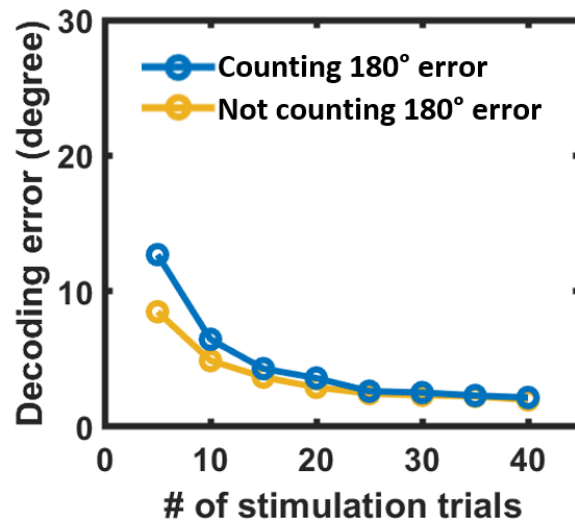
Supplementary Fig. 2 | Representative spike raster showing distinct responses to grating stimulus. A-G show responses to light on/off. H-N show responses to stimulus at around 400 ms after stimulation onset. O-U show responses to stimulus at around 250-350 ms after stimulation onset.



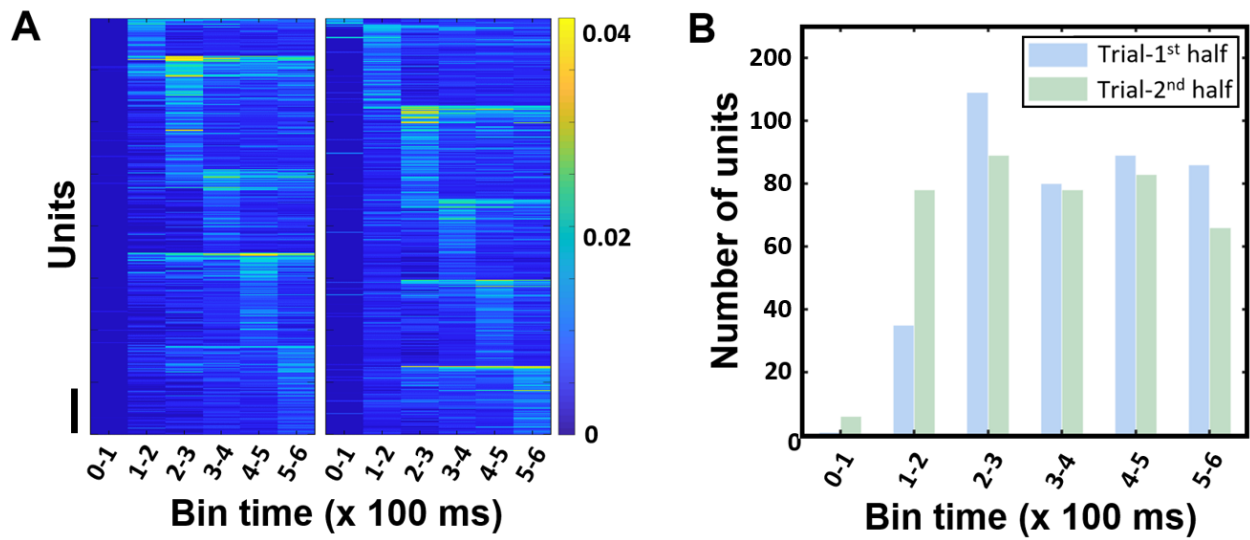
Supplementary Fig. 3. The peak firing time of active units at all angles. The peak firing times of the most active 30% of units with stimuli of 24 orientations of drifting grating. The units are plotted according to their estimated positions and color coded by time after stimulus onset.



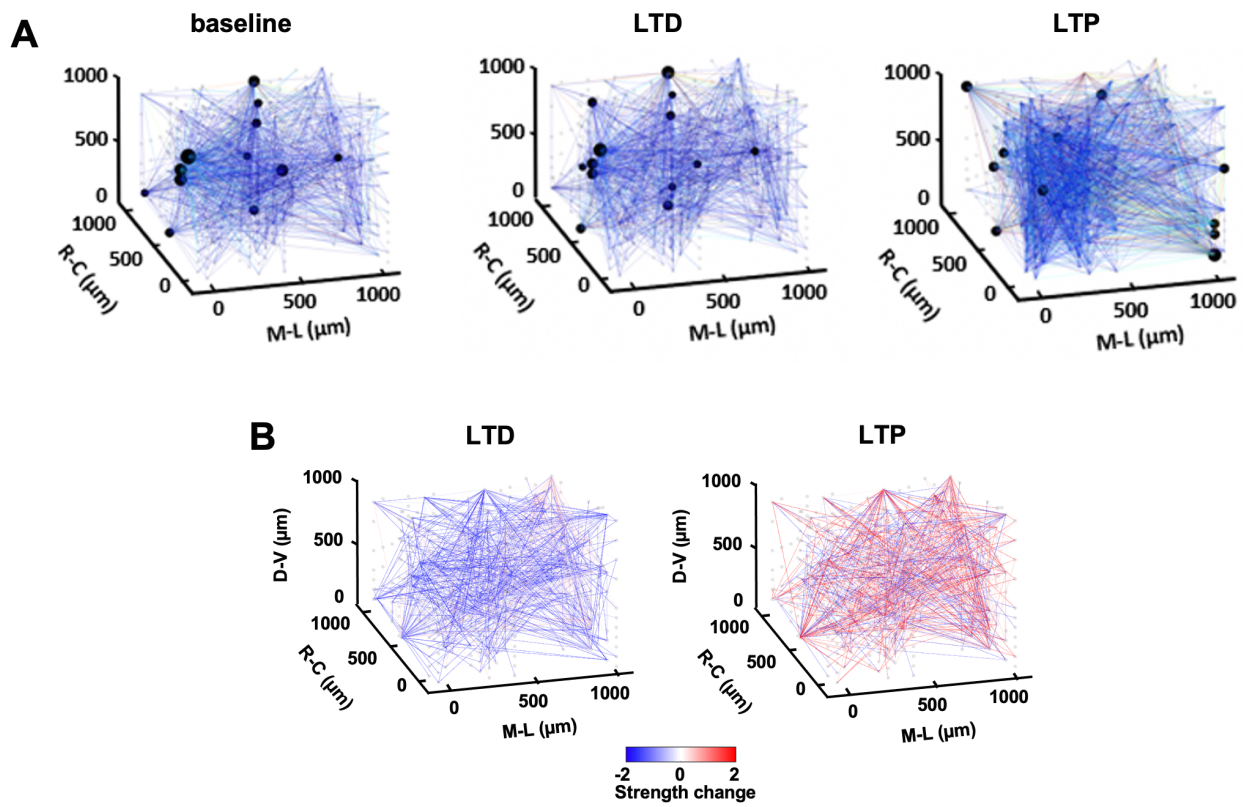
Supplementary Fig. 4 | Comparison of the correlation distributions computed using all units Vs single units. The strength, latency, and distance of correlation between all unit pairs have similar distributions as those between single unit pairs. Purple indicates with visual stimuli and red indicates without.



Supplementary Fig. 5 | Scaling of the decoding error with the number of trials. Subsets of randomly selected stimulation trials were used for training with all 1355 units.



Supplementary Fig. 6 | Distributions of unit prediction power. (A), Prediction power of Top 30% most predictive units were ranked by in which time bin after stimulus onset they were most predictive. (Left: 1st half trials. Right: 2nd half trials). Scale bar: 250. (B), Distribution of best prediction time for top 30% most predictive units.



Supplementary Fig. 7 | Pair-wise coupling map showing the change induced by LTD and LTP optogenetic stimulation protocols. (A), Spatial distribution of the “super nodes” (black dots) in the pair-wise connectivity at no stimulation and under LTD, LTP stimulation protocols. **(B),** Pair-wise coupling strength change introduced by optical LTD and LTP protocols relative to baseline.

Supplementary Video 1

An ultraflexible 128-channel NET array floating in water. The vigorous motions were induced by nearby water drops.

Supplementary Video 2

MicroCT scan of a NET array implanted in approximately 1 mm³ cortical tissue of a mouse brain, consisting of eight 128-channel modules, 1024 recording sites in total.

Supplementary Video 3

Example 3D reconstruction of local field potentials recorded by a 1024-channel NET array. Video is played at 0.1× real time.

Supplementary Video 4

Example spiking activity recorded in visual regions responding to drifting grating stimuli. The darker region represents primary visual cortex (V1). Video is played at 0.2× real time.

Supplementary Video 5

Example spiking activity recorded in visual, sensory and motor cortical regions. Video is played at 0.1× real time.

Supplementary Video 6

Example local field potentials recorded in visual, sensory and motor cortical regions. Video is played at 0.1× real time.

Supplementary Video 7

Example video of animals' facial motions was compressed and deconstructed into 8 latent variables using a convolutional autoencoder (top). The video was reconstructed by predicted variables using recorded neural activity (middle). The residual (bottom) represents the prediction error.